Bulgarian Chemical Communications, Volume 56, Issue 2 (pp. 169-174) 2024 *DOI: 10.34049/bcc.56.2.SPSCBT-06*

Preparation and antimicrobial activity of silver nanoparticles impregnated with halloysite clay

K. L. Zaharieva[1*], R. T. Eneva[2], S. L. Mitova[2], O. S. Dimitrov[3], H. P. Penchev[4]

[1]*Institute of Mineralogy and Crystallography "Acad. I. Kostov", Bulgarian Academy of Sciences, Acad. G. Bonchev Str., Bl. 107, 1113 Sofia, Bulgaria*
[2]*The Stephan Angeloff Institute of Microbiology, Bulgarian Academy of Sciences, Acad. G. Bonchev Str., Bl. 26, 1113, Sofia, Bulgaria*
[3]*Institute of Electrochemistry and Energy Systems, Bulgarian Academy of Sciences, Acad. G. Bonchev Str., Bl. 10, 1113 Sofia, Bulgaria*
[4]*Institute of Polymers, Bulgarian Academy of Sciences, Acad. G. Bonchev Str., Bl.103A, 1113 Sofia, Bulgaria*

Received: February 08, 2024; Revised: May 10, 2024

In the present work, nanotubular halloysite clay was ultrasonically treated and impregnated with silver nanoparticles. The citrate surface-stabilized silver nanoparticles dispersion was prepared using an effective method of electrochemical synthesis. The elemental and phase composition, and the structure of the obtained AgNPs-impregnated and pristine halloysite were investigated by various methods such as X-ray fluorescence (XRF), powder X-ray diffraction analyses and Fourier-transform infrared spectroscopy. The Ag-loaded halloysite sample with 0.454 wt.% silver content was confirmed by the XRF analysis. The antimicrobial activity of the pristine and the AgNPs-impregnated halloysite clay was tested against *Escherichia coli* ATCC 25922 (Gram-negative) and *Bacillus subtilis* ATCC 6633 (Gram-positive) strains. The results show that pure halloysite does not exhibit antibacterial activity. The AgNPs-impregnated halloysite demonstrates antibacterial activity against *Escherichia coli* and *Bacillus subtilis* with only bacteriostatic effect.

Keywords: halloysite, silver nanoparticles, antimicrobial activity, *Escherichia coli, Bacillus subtilis*

INTRODUCTION

Halloysite nanotubes (HNTs) are clay minerals that belong to the kaolin group of clays. They have been widely investigated due to their interesting structure and properties in recent decades. HNTs are dioctahedral 1:1 clay minerals present in soils. This mineral can be found worldwide, in particular in wet tropical and subtropical regions and weathered rocks. Countries such as Belgium, China, New Zealand and France are rich in this clay [1]. The empirical chemical formula of halloysite nanotube aluminosilicate clay is $Al_2Si_2O_5(OH)_4.2H_2O$ [2]. Halloysite consists of hollow cylinders formed by multiple rolled alumino-silicate layers [3]. It is present in two forms, the hydrated form (Halloysite-10 Å) and the dehydrated one (Halloysite-7 Å) [4]. Halloysite-based nano-composites have attracted attention as a potential material for various biological applications as enzyme and antibacterial immobilization, controlled drug delivery, etc. [3]. The profound scientific interest in both natural and synthetic HNTs clays could be attributed to their unique physico-chemical properties: their nanotubular structures, length-to-diameter (L/D) ratio, high specific surface area, hydrophobicity and intercalating properties [3, 5].

The antibacterial application of halloysite-halloysite-based nanocomposites containing different metal nanoparticles such as Ag, Cu, Au, Fe, and Ag-Cu bimetallic nanoclusters or metal oxides (ZnO, Fe_3O_4, CeO_2, MnO_x) has been studied by many research groups [3, 6-15]. In human daily life, antibacterial agents and nanocomposite materials are widely used and effectively help in society health shielding by preventing the transmission of many existing pathogens and the corresponding infectious diseases. Lately, antibacterial properties of transition metal nanomaterials have become increasingly attractive areas of research, including silver nanoparticles, silver nanorods, copper nanoparticles, etc. Among them, silver attracts attention since it is strongly active against a broad spectrum of fungal and bacterial species, and displays low toxicity, low volatility and high thermal stability. It is also effective against antibiotic-resistant strains of microorganisms [6].

The present paper aims at preparing AgNPs-impregnated halloysite clay. An effective electrochemical method was used for the preparation of citrate surface stabilized concentrated silver nanoparticles dispersion. The phase and elemental composition, and the structure of the AgNPs-impregnated halloysite and pristine halloysite were

* To whom all correspondence should be sent:
E-mail: *zaharieva@imc.bas.bg*

determined using different physicochemical methods. The antimicrobial activity of AgNPs-impregnated halloysite against pathogens *E. coli* and *B. subtilis* was studied as well.

EXPERIMENTAL

Preparation of AgNPs- impregnated halloysite material

The halloysite nanoclay ($(H_4Al_2O_9Si_2.2H_2O)$, M = 294.12 $g.mol^{-1}$) from Sigma-Aldrich was impregnated with a citrate surface-stabilized Ag nanoparticles dispersion. Silver nanoparticles dispersion with total silver concentration of 400 $mg.L^{-1}$ was synthesized using a slightly modified methodology proposed in [16]. The electrochemical reduction method used square-shaped bulk silver (probe 999) electrodes as metal source, 47 V applied DC voltage and dissolved sodium citrate (500 $mg.L^{-1}$) as surface stabilizing agent. The advantage of the electrochemical method is the purity of the obtained colloidal silver and there is no need to purify the product from residual salts as in the case of chemical reduction methods. The impregnation was performed using ultrasonic treatment of 2.1 g of halloysite and 30 ml of AgNPs colloidal dispersion (400 ppm) for 10 minutes followed by stirring (500 rpm) for 5 hours at 50°C using a magnetic stirrer. After that, the AgNPs-impregnated halloysite was filtered and washed several times with distilled water until neutral reaction and the resultant pale-brown fine powder was dried for 1 hour at 50°C in a vacuum oven (Figure 1).

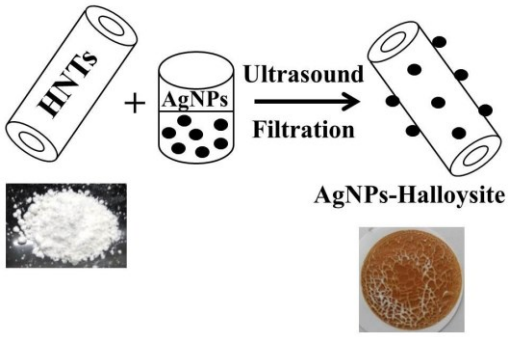

Fig. 1. Preparation of AgNPs-impregnated halloysite hybrid.

Physicochemical characterization

The phase and elemental composition, and the structure of the obtained AgNPs-impregnated halloysite material and the pristine halloysite were determined by powder X-ray diffraction analyses, X-ray fluorescence (XRF) and Fourier-transform infrared spectroscopy (FT-IR). The powder X-ray diffraction analysis (PXRD) of the investigated samples was performed on an X-ray powder diffractometer "Empyrean" within the range of 2θ values between 2° and 70° using Cu Kα radiation (λ = 0.154060 nm) at 40 kV and 30 mA. The phases in the prepared materials were established using the ICDD database. Wave-dispersive X-ray fluorescence (WDXRF) analyses were performed using a Supermini 200 spectrometer (Rigaku, Osaka, Japan). Data collection was performed by wave-dispersed X-ray fluorescence at 50 kV and 4.0 mA. Data processing was performed using the ZSX software package. The analysis used a semi-quantitative method to determine the elemental composition. The results obtained by the method of semi-quantitative analysis "SQX" allow the determination of the chemical composition of samples without the need for comparative materials (standards). The FT-IR spectra of the prepared materials were recorded on a Bruker Tensor 37 spectrometer in the region 4000–400 cm^{-1}, using the KBr pellet technique. The surface morphology of the samples was investigated by scanning electron microscopy (SEM) using Zeiss Evo 10 microscope (Carl Zeiss Microscopy, Oberkochen, Germany). TEM analyses were carried out on an HR STEM JEOL JEM 2100.

Antimicrobial activity

Materials and methods. Escherichia coli ATCC 25922 (Gram-negative, G-) and *Bacillus subtilis* ATCC 6633 (Gram-positive, G+) were used as test microorganisms. Overnight cultures in Mueller-Hinton Broth were diluted to approx. 5×10^5 colony forming units (CFU)/mL.

The antimicrobial activity of the materials was evaluated by the drop dilution method in a 96-well sterile plate, in the presence of resazurin [17]. Resazurin dye indicates cell viability by changing colour from blue to pink upon chemical reduction resulting from aerobic respiration of growing cells. Halloysite and Ag-halloysite were tested in two-fold decreasing concentrations from 20 to 0.312 mg/mL. The lowest concentration of nanoparticle suspension that inhibited cell growth (dye did not convert to pink) was defined as the minimum inhibitory concentration (MIC).

Gentamycin for *E. coli* in concentrations from 0.5 to 0.008 mg/mL and erythromycin for *B. subtilis* in concentrations from 20 to 0.312 mg/mL were used as positive controls.

RESULTS AND DISCUSSION

The recorded powder X-ray diffraction patterns of pristine halloysite and AgNPs-impregnated halloysite are presented in Figure 2A.

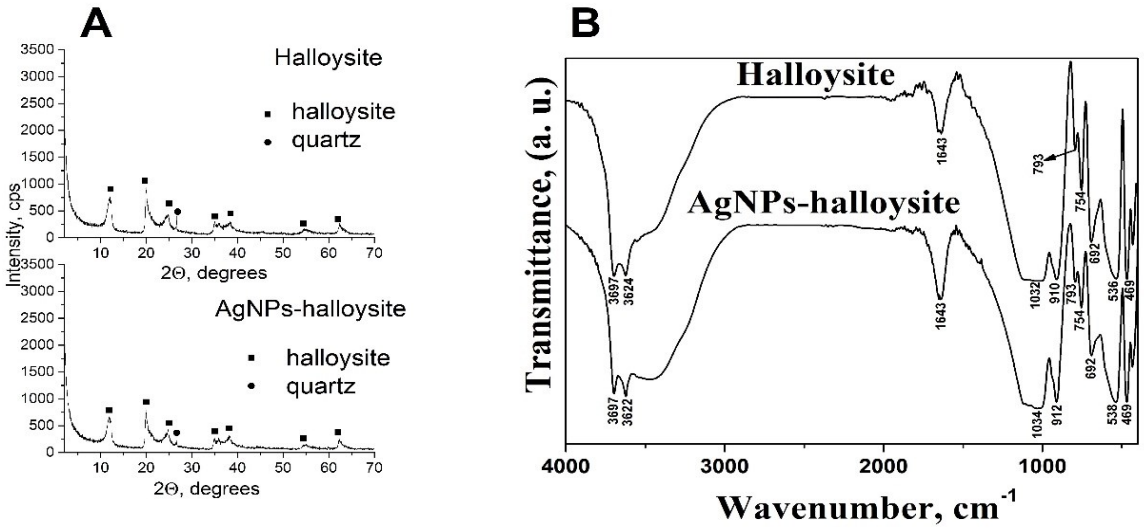

Fig. 2. A) PXRD patterns of pristine halloysite and AgNPs-impregnated halloysite and **B)** FT-IR spectra of pure halloysite and AgNPs-impregnated halloysite.

Table 1. Elemental composition (wt.%) of pristine halloysite and AgNPs-impregnated halloysite, determined by XRF analysis.

Sample	Si/Al (wt. ratio)	Ag	Al	Si	P	S	K	Ca	Ti	Fe	Ni	Zn
AgNPs-impregnated halloysite	0.68	0.454	38.1	55.7	2.17	0.175	0.193	1.52	0.222	1.36	0.0836	-
halloysite	0.68	-	38.0	56.1	2.15	0.217	0.294	1.46	0.218	1.33	0.0847	0.0228

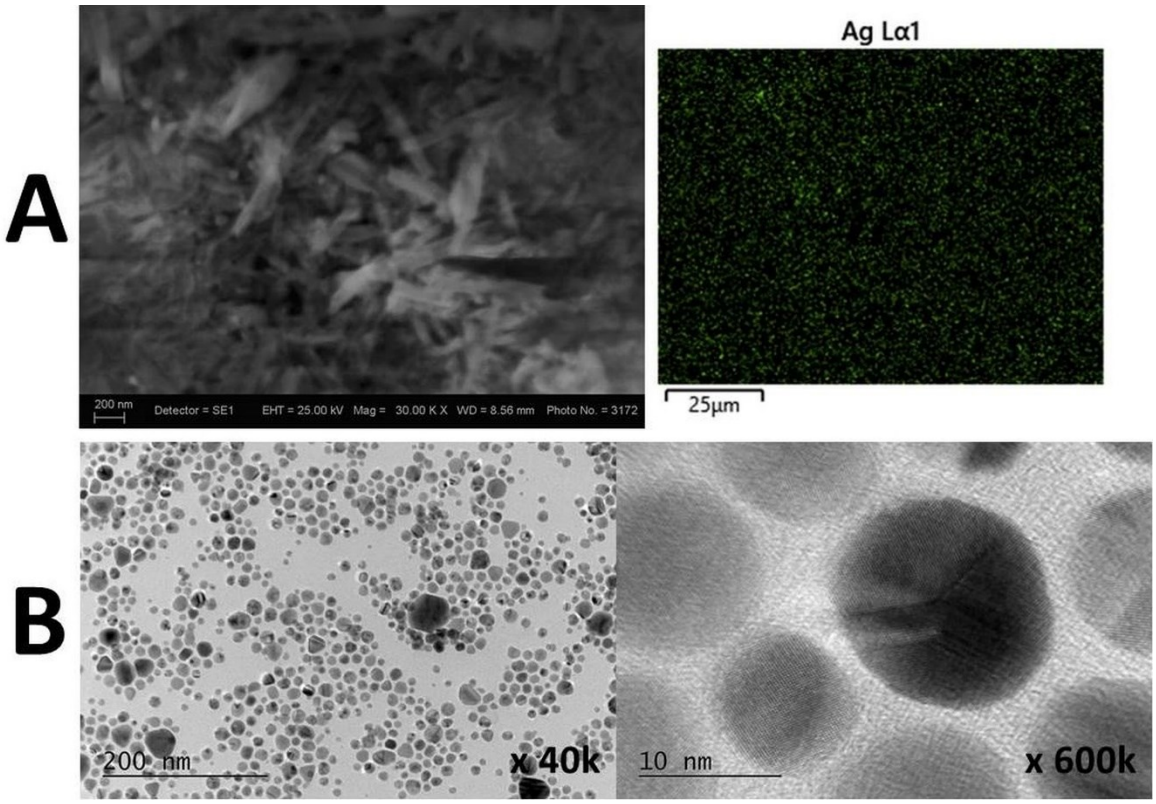

Fig. 3. A) SEM images of AgNPs-impregnated halloysite and **B)** TEM images of AgNPs.

The powder X-ray diffraction analysis of the investigated samples pointed to the presence of halloysite phase (PDF-00-009-0453) in AgNPs-impregnated and pure halloysites. A reflection peak corresponding to the small content of quartz (PDF-00-033-1161) was also found. The silver phase was not established owing to its small amount below the sensitivity threshold. The PXRD results show that the modification of halloysite with silver nanoparticles does not lead to observable structural changes.

The XRF data are displayed in Table 1. The silver content in the AgNPs-impregnated halloysite material is 0.454 wt.%. The Si/Al ratios in the investigated halloysite materials are preserved after impregnation with silver nanoparticles. The results from XRF and PXRD analyses show that after the impregnation, the halloysite structure is retained. Similar structure retention referred to the halloysite clay mineral after impregnation with Cu and Co oxides was established by another research group [18].

Figure 2B shows the FT-IR spectra of the investigated samples. The bands at 3697 cm^{-1} and 3622-3624 cm^{-1} correspond to OH stretching vibrations attributed to the inner surface and inter-layer hydroxyl groups of halloysite clay. A characteristic peak was recorded at 1643 cm^{-1} due to the O-H vibration of adsorbed water on the halloysite surface [19]. The bands at wavenumbers 1032-1034 cm^{-1} and 910-912 cm^{-1} were assigned to the stretching vibrations of Si-O-Si and bending modes of Al-O-H [20, 21]. The vibrations observed at 754 and 692 cm^{-1} are due to perpendicular Si–O stretching [21]. The band observed at 793 cm^{-1} was attributed to the symmetric stretching of Si-O. The peaks at 536-538 and 469 cm^{-1} were attributed to the deformation of both Al-O-Si and Si-O-Si [22]. The data determined by FT-IR spectroscopy are in agreement with results established using powder X-ray diffraction and XRF analyses. The presence of spherical AgNPs with average particle diameter about 20 nm on the surface of tubular shaped halloysite is observed using SEM and TEM studies (Figures 3A and 3B).

Clays are materials with wide application for health purposes, because they are natural, easily available, biocompatible, low-cost, capable of crossing cellular membranes [23]. Some authors assume that, in contrast to other clays, halloysite itself is not considered an antibacterial material. Depending on the goal, it can be used both to maintain a given microbial population and as a carrier of ions or substances with antimicrobial action [24]. On the other hand, Abhinayaa *et al*. [25] compared the antibacterial activity of pristine halloysite with that of halloysite modified with various surfactants and reported inhibition of phytopathogenic G- bacteria at 2.5 mg/mL for halloysite and at 0.3-1.25 mg/mL for its modified forms. In our study, pristine halloysite showed no antibacterial activity, even at a concentration of 20 mg/mL. The AgNPs-loaded form of halloysite displayed inhibitory activity against the tested bacteria at concentrations of 0.312 mg/mL for *E. coli* and 1.25 mg/mL for *B. subtilis* (Figures 4-6).

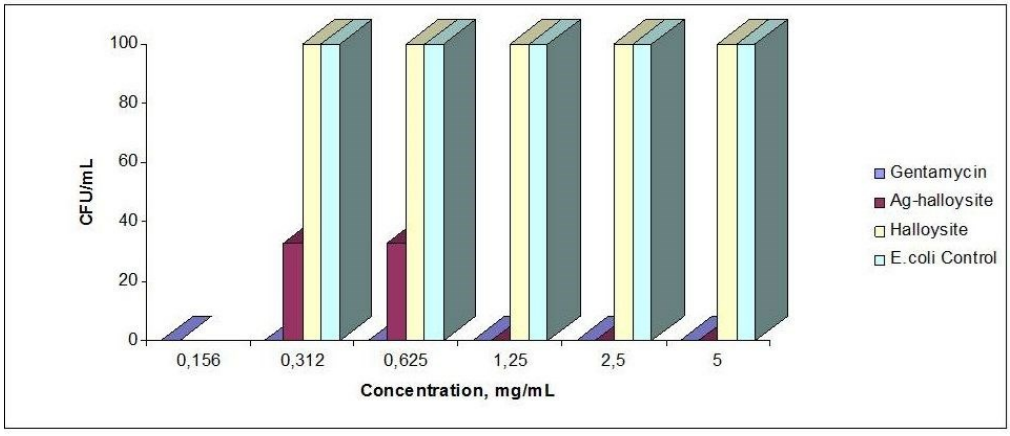

Fig. 4. Antimicrobial activity of AgNPs-impregnated halloysite against *E. coli* ATCC 25922 compared to halloysite.

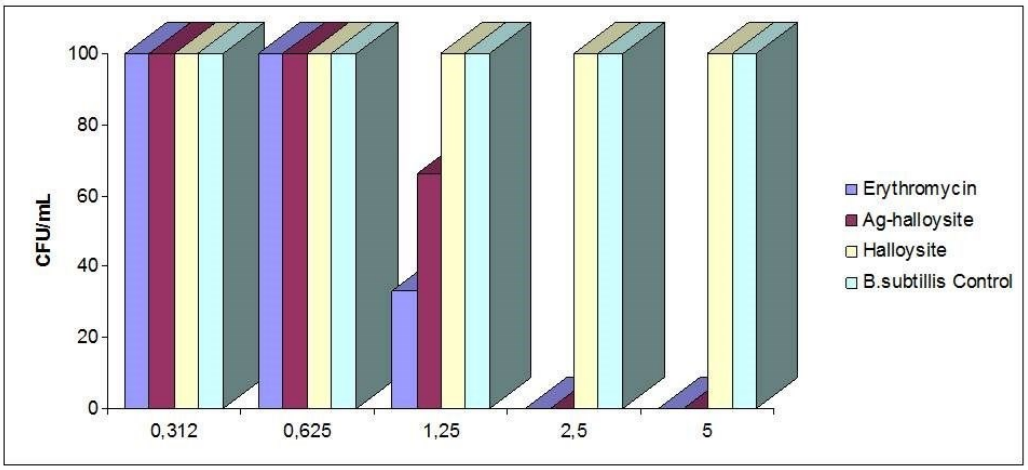

Fig. 5. Antimicrobial activity of AgNPs-impregnated halloysite against *B. subtilis* ATCC 6633 compared to halloysite.

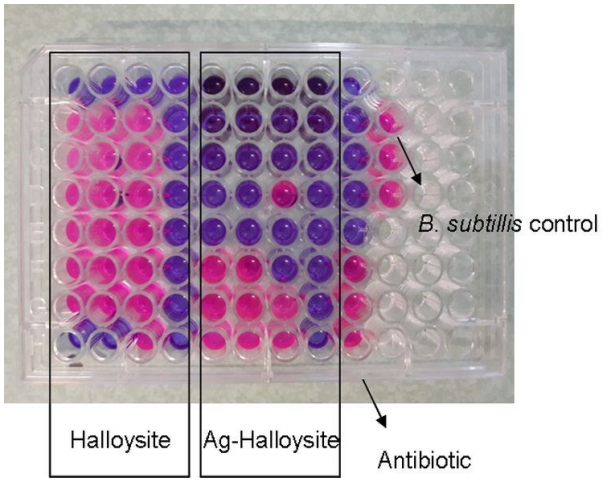

Fig. 6. Drop dilution method in a 96-well sterile plate, according to Sarker *et al*. [17]. Antimicrobial activity of halloysite and AgNPs-impregnated halloysite was tested in decreasing concentrations from 20 to 0.312 mg/mL. Wells in magenta contain inhibited bacterial culture; wells in pink contain growing bacteria. The antibiotic tested is erythromycin in the same decreasing concentrations.

These results indicate that the suppressive action is due to the silver nanoparticles. After inoculation on a solid medium of the bacterial cultures containing silver nanoparticles-impregnated halloysite at these concentrations, only a reduction in the number of CFU was observed, and not a lack of growth, which means that the action of silver nanoparticles-impregnated halloysite on the tested strains is bacteriostatic. Both G- and G+ bacteria have a negative charge on the cell surface, suggesting an electrostatic interaction with the positively charged nanoparticles and adhesion on the bacterial cell [24]. This could cause structural changes or functional damage, due to the production of oxygen radicals catalyzed by silver ions [6], which leads to an imbalance in the redox potential of bacterial cells. In our study, the G+ test strain shows higher resistance. The mechanism of interaction between the prepared AgNPs-impregnated halloysite and the bacterial cells, as well as the ability of *B. subtilis* to tolerate higher concentrations of silver nanoparticles are to be elucidated by further studies. The prepared AgNPs-impregnated halloysite material could find possible applications as antibacterial filter for treatment of contaminated waters and as potential catalyst for oxidation of CO to CO_2.

CONCLUSIONS

The silver-impregnated halloysite material was successfully prepared using silver nanoparticles obtained by the electrochemical reduction method. The presence of 0.454 wt.% of silver in the AgNPs-impregnated halloysite sample was determined by XRF analysis. The results from the PXRD analyses show that after the impregnation, the halloysite structure is preserved. Silver-impregnated halloysite demonstrated inhibitory activity against *E. coli* and *B. subtilis* at concentrations of 0.312 and 1.25 mg/mL, respectively. A good antimicrobial activity towards *E. coli* bacteria was displayed by the silver-impregnated halloysite sample. The *B. subtilis* test strain showed higher resistance. The effect of Ag-loaded halloysite against *E. coli* and *B. subtilis* is bacteriostatic. Comparison with pristine halloysite shows that the suppressive action is due to the silver nanoparticles.

Acknowledgement*: The authors acknowledge the technical support from the project PERIMED BG05M2OP001-1.002-0005/29.03.2018 (2018–2023). H.P. thanks to the National Infrastructure NI SEVE supported by the Bulgarian Ministry of Education and Science under grant agreement N° Д01-385/Д01-18.12.2020. Thanks are due to Liliya*

Tsvetanova for her technical assistance in the XRF analysis.

REFERENCES

1. M. Massaro, R. Noto, S. Riela, *Molecules*, **25**, 4863 (2020).
2. M. J. Saif, H. M. Asif, M. Naveed, *J. Chil. Chem. Soc.,* **63**, 4109 (2018).
3. Z. Shu, Y. Zhang, Q. Yang, H. Yang, *Nanoscale Res. Lett.,* **12**, 135 (2017).
4. P. Lampropoulou, D. Papoulis, *Materials,* **14**, 5501 *(*2021).
5. Y. Zhao, E. Abdullayev, A. Vasiliev, Y. Lvov, *J. Colloid Interface Sci.,* **406**, 121 (2013).
6. Y. Zhang, Y. Chen, H. Zhang, B. Zhang, J. Liu, *J. Inorg. Biochem.,* **118**, 59 (2013).
7. S. Jana, A. V. Kondakova, S. N. Shevchenko, E. V. Sheval, K. A. Gonchar, V. Y. Timoshenko, A. N. Vasiliev, *Colloids Surf. B: Biointerfaces,* **151**, 249 (2017).
8. A. R. Sayfutdinova, K. A. Cherednichenko, A. A. Bezdomnikov, U. P. Rodrigues-Filho, V. V. Vinokurov, B. Tuleubayev, D. Rimashevskiy, D. S. Kopitsyn, A. A. Novikov, *JCIS Open*, **12**, 100098 (2023).
9. X. Ding, H. Wang, W. Chen, J. Liu, Y. Zhang, *RSC Adv.,* **4**, 41993 (2014).
10. X. Xu, Y. Chao, X. Ma, H. Zhang, J. Chen, J. Zhu, J. Chen, *Int. J. Biol. Macromol.,* **258**, 128704 (2024).
11. J. Cervini-Silva, A. N. Camacho, E. Palacios, P. Angel, M. Pentrak, L. Pentrakova, S. Kaufhold, K. Ufer, M. T. Ramírez-Apan, V. Gómez-Vidales, D. R. Montaño, A. Montoya, J. W. Stucki, B. K. G. Theng, *Appl. Clay Sci.,* **120**, 101 (2016).
12. Y. Jin, F. Zhang, J. Fan, H.-J. S. Fan, *Appl. Clay Sci.,* **231**, 106750 (2023).
13. S.-C. Jee, M. Kim, S. K. Shinde, G. S. Ghodake, J.-S.Sung, A. A. Kadam, *Appl. Surf. Sci.,* **509**, 145358 (2020).
14. Z. Shu, Y. Zhang, J. Ouyang, H. Yang, *Appl. Surf. Sci.,* **420**, 833 (2017).
15. J. Wang, S. Wu, W. Zhang, H. Wang, P. Zhang, B. Jin, C. Wei, R. Guo, S. Miao, *Appl. Clay Sci.,* **216**, 106352 (2022).
16. S. Sharma, K. Choudhary, I. Singhal, R. Sain, *Int. J. Pharm. Sci. Rev. Res.,* **28**, 272 (2014).
17. S. D. Sarker, L. Nahar, Y. Kumarasamy, *Methods,* **42**, 4 (2007).
18. A. M. Carrillo, J. G. Carriazo, *Appl. Catal. B: Environ.,* **164**, 443 (2015).
19. S. S. Abdullahi, N. H. Hanif Abu Bakar, A. Iqbal, N. H. Yusof, *Egypt. J. Chem.,* **66**, 345 (2023).
20. H. Cheng, R. L. Frost, J. Yang, Q. Liu, J. He, *Spectrochim. Acta A Mol. Biomol. Spectrosc.,***77**, 1014 (2010).
21. Y. Zheng, L. Wang, F. Zhong, G. Cai, Y. Xiao, L. Jiang, *Ind. Eng. Chem. Res*., **59**, 13, 5636 (2020).
22. P. Yuan, P. D. Southon, Z. Liu, M. E. R. Green, J. M. Hook, S. J. Antill, C. J. Kepert, *J. Phys. Chem. C,* **112**, 15742 (2008).
23. M. Notarbartolo, M. Massaro, R. de Melo Barbosa, C. Emili, L. F. Liotta, P. Poma, F. M. Raymo, R. Sànchez-Espejo, R. Vago, C. Viseras-Iborra, S. Riela, *Colloids Surf. B Biointerfaces*, **220**, 112931 (2022).
24. O. P. Setter, E. Segal, *Nanoscale***, 12**, 23444 (2020).
25. R. Abhinayaa, G. Jeevitha, D. Mangalaraj, N. Ponpandian, P. Meena, *Appl. Clay Sci.*, **174**, 57 (2019).